Shear Flow Induced Orientation Development during Homogeneous Solution Polymerization of Rigid Rodlike Molecules

U. S. Agarwal† and D. V. Khakhar*

Department of Chemical Engineering, Indian Institute of Technology—Bombay, Powai, Bombay 400076, India

Received January 28, 1993; Revised Manuscript Received April 27, 1993

ABSTRACT: The dynamic variation of optical birefringence during solution polycondensation of rigid rodlike molecules in a simple shear flow is obtained. At relatively high shear rates (413 s^{-1}) and late stages of the polymerization the orientation of the molecules is found to be significant. Molecular orientation is important in such reactions since it increases the polymerization rate and alters the molecular weight distribution (Agarwal, U. S.; Khakhar, D. V. *Nature* **1992**, *360*, 53). The birefringence at different shear rates ($\dot{\gamma}$) over the course of the polymerization is found to depend only on $\dot{\gamma}/D_r$, where D_r is the rotational diffusivity. The predictions of the theory of Marrucci and Grizzuti (*J. Polym. Sci., Polym. Lett. Ed.* **1983**, *21*, 83), however, show large deviations in comparison to the experimental birefringence measurements. The experiments are carried out using terephthaloyl chloride and *p*-phenylenediamine to produce poly(*p*-phenyleneterephthalamide) in a mixed solvent at low temperatures. A two-reactor system is used in which the second reactor is designed to give a uniform simple shear flow and to allow for measurement of birefringence during polymerization.

1. Introduction

Rigid rodlike (RRL) polymers are technologically of considerable importance because they form liquid crystalline solutions and these solutions can be processed into thermally stable, high-modulus and high-strength fibers. Such properties arise during their processing due to the rigidity and the large axis to diameter ratio of the RRL molecules, which enhances their orientational response to flow fields. Hence orientation during processing is of practical interest and is the subject of several previous studies.[1-8]

Orientation of the molecules may play an important role during the polymerization process as well. All previous investigations of the kinetics of solution polycondensation of RRL molecules show that after an initial period, during which the polymerization is relatively rapid, the rate constant decreases by an order of magnitude and the molecular weight increases very slowly with time.[9-11] The decrease in rate of reaction is attributed to rotational diffusional limitations when the molecules become long enough.[9,11,12] In the semidilute regime (defined by $\nu = \rho L^3 \gg 1$, where ρ is the number concentration and L is the length of the molecule), the rotational diffusivity decreases sharply with molecular length ($D_r \sim L^{-7}$)[13] and the rate of generation of molecular pairs which satisfy the criteria for reaction (proximity of reactive end groups and near-parallel alignment of molecules) becomes very low. Vigorous stirring during such polymerization is found to be necessary to obtain high molecular weights,[14,15] and the type of mixer used for polymerization affects the limiting molecular weight.[16] In a recent experimental study[11] of the polymerization of poly(*p*-phenyleneterephthalamide) (PPTA) in a simple shear flow we observed a significant increase in the polymerization rate with flow at the later stages of the reaction. Simultaneous measurement of birefringence showed that the orientation of the molecules by flow was also significant at this stage. Such molecular orientation increases (i) the fraction of molecular pairs likely to react (since molecules must be aligned nearly parallel to each other prior to reaction[17]) and (ii) the rotational diffusivity of the molecules.[13] Both factors would result in an increase in the rate of reaction. Higher rates of polymerization imply higher limiting molecular weights in the presence of competing side reactions[18,19] which cap the end groups. In addition, the molecular weight distribution is affected because of the different rates of reaction of the molecules of different lengths.[11]

In this work we have carried out a study of kinetics and molecular orientation, using optical birefringence during the solution polymerization of PPTA in the presence of a simple shear flow. The results are interpreted using the theory of Doi and Edwards (DET)[13] and its extension for polydisperse cases by Marrucci and Grizzuti,[20] referred to as the DEMG theory.[6] The primary objective of the study is to obtain a better understanding of the role of shearing in the polymerization of RRL molecules, which is of considerable practical importance.

In the following sections we first present a brief review of the rotational dynamics of RRL polymers in solutions experiencing a simple shear flow and their relation to birefringence. The polymerization procedure and birefringence measurements are detailed in section 3. Results and discussion are given in section 4, and the conclusions of the study in section 5.

2. Theory

Doi and Edwards[13] showed that the steady-state orientation distribution under a shear flow depends on only one dimensionless parameter, $\dot{\gamma}/D_r$, if the rotational diffusivity is only a function of the shear rate ($\dot{\gamma}$). At $\dot{\gamma}/D_r \geq 1$, alignment of molecules along the flow direction takes place, and the orientation distribution can be derived from the rotational dynamics. This can be related to the flow birefringence (Δ), caused by the anisotropy in polarizability of RRL molecules. The polarizability of RRL molecules is proportional to length; i.e., there is a constant polarizability per unit length. Hence, for a given level of orientation, the birefringence of a solution is independent of molecular lengths and is proportional to c, the weight concentration.[21] For a given system, if Δ is normalized with respect to c and plotted against $\dot{\gamma}/D_r$ then steady-state data for the system should fall on a master curve

$$\Delta/c = Mf(\dot{\gamma}/D_r) \tag{2.1}$$

where M is a constant related to the intrinsic polarizability

* Author to whom all correspondence should be addressed.
† Current address: Chemical Engineering Division, National Chemical Laboratory, Pune 411008, India.

0024-9297/93/2226-3960$04.00/0

of the repeat unit. This has been verified experimentally for systems of constant molecular weight for various $\dot{\gamma}$ and c.[7,8]

During step-growth polymerization, a distribution of rod lengths (L_i) exists. The variation of the orientation distribution function $f_i(\mathbf{u},t)$ for molecules of length L_i for this case is given by[6,13,22]

$$\frac{\partial f_i}{\partial t} = \nabla_u\cdot\tilde{D}_{ri}\left(\nabla_u f_i + \frac{f_i}{k_B T}\nabla_u V\right) + \nabla_u\cdot(\dot{\mathbf{u}}f_i) + R_i^g - R_i^c \quad (2.2)$$

where $\mathbf{u}$ is the unit vector along the rod axis, $\tilde{D}_{ri}$ is the rotational diffusion coefficient of the rod under flow conditions, and ∇_u is the gradient operator on the sphere $|\mathbf{u}| = 1$. R_i^g and R_i^c are contributions from generation and consumption due to the polymerization reaction, k_B is the Boltzmann constant, and T is the solution temperature. $V(\mathbf{u})$ is the mean field potential acting on the rod due to surrounding rods, and

$$\dot{\mathbf{u}} = \mathbf{k}\cdot\mathbf{u} - (\mathbf{u}\cdot\mathbf{k}\cdot\mathbf{u})\mathbf{u} \quad (2.3)$$

where k is the velocity gradient tensor of the applied flow field.

In the case of interest, the change in f_i due to the generation and consumption of molecules by reaction (time scale $\sim$ 1 min) is very slow as compared to the approach of f_i to equilibrium driven by the diffusion and flow terms (time scale $\sim$0.01 s). Thus, we apply a quasi-steady-state assumption to eq 2.2, use the preaveraged diffusivity ($\tilde{D}_{ri}$), and neglect intermolecular interactions to get

$$\tilde{D}_{ri}\nabla_u\cdot\nabla_u f_i + \nabla_u\cdot(\dot{\mathbf{u}}f_i) = 0 \quad (2.4)$$

Doi and Edwards[13] first solved this for the orientation distribution for steady-state simple shear flow of a monodisperse system by the method of infinite series expansions. Based on its extension to the polydisperse case by Marrucci and Grigguti,[20] Chow and Fuller[6] presented a procedure for obtaining the orientation distribution for such systems under shear flow. We briefly review the results of the theory below.

Expanding f_i in spherical harmonics

$$f_i = \sum_{l=2,4}^{\infty}\sum_{m=0}^{l} b_{lm,i}|lm\rangle \quad (2.5)$$

and substitution in eq 2.4 yields the following system of equations for each set of coefficients $b_{lm,i}$

$$\mathbf{A}\cdot\mathbf{b}_i - (\dot{\gamma}/\tilde{D}_{ri})\mathbf{B}\cdot\mathbf{b}_i = (\dot{\gamma}/\tilde{D}_{ri})\mathbf{d} \quad (2.6)$$

where

$$A_{lm,l'm'} = \begin{cases} l(l+1) & \text{if } l = l' \text{ and } m = m' \\ 0 & \text{otherwise} \end{cases}$$

$$B_{lm,l'm'} = (lm|\Gamma|l'm')$$

$$d_{lm} = (lm|\Gamma|00)(1/4\pi)^{1/2}$$

for $m = 1, 2, \ldots, l$, $l = 2, 4, \ldots, l_{max}$. The operator $|\Gamma|$ and the matrix elements $(lm|\Gamma|l'm')$ are defined in ref 13. The individual preaveraged rotatonal diffusivities for an anisotropic orientation distribution are

$$\tilde{D}_{ri} = \beta' L_i^{-4}\left(\sum_n \rho_n L_n Q_{in}\right)^{-1}\left(\sum_{j\le i}\rho_j L_j^4 Q_{ij} + L_i^3\sum_{j>i}\rho_j L_j Q_{ij}\right)^{-1} \quad (2.7)$$

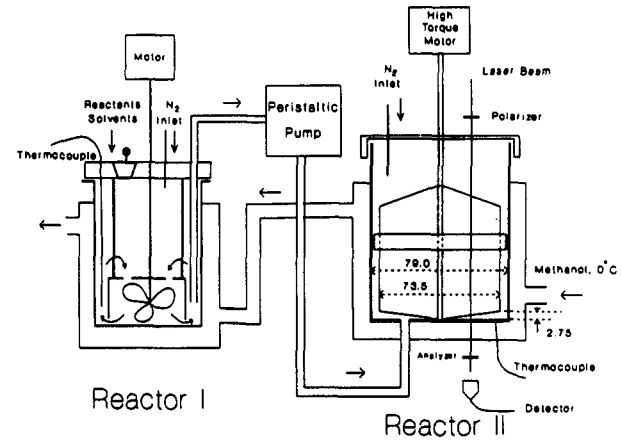

Figure 1. Schematic view of apparatus for polymerization. Reactor dimensions shown are in millimeters.

where

$$Q_{ij} = 1 - 8\pi\sum_{l=2,4}^{\infty}\sum_{m=0}^{l}\frac{l-1}{l+2}\left(\frac{(l-3)!!}{l!!}\right)^2 b_{lm,i}b_{l'm',i} \quad (2.8)$$

and the double factorials are defined[23] as

$$(2n)!! = (2n)(2n-2)(2n-4)\ldots4\cdot2$$

$$(2n+1)!! = (2n+1)(2n-1)(2n-3)\ldots3\cdot1$$

$\beta' = \beta(3k_BT/\pi\eta_s)$, η_s is the solvent viscosity, and the factor β corresponds to corrections in the original DET for incomplete caging up to $\nu = \nu^* \sim 40$.[22]

The birefringence Δ_{13} is related to the moments of f_i by[6,24]

$$\Delta_{13} = M\sum_i \rho_i L_i\langle u_1^2 - u_3^2\rangle_i \quad (2.9)$$

with

$$\langle u_1^2 - u_3^2\rangle_i = 2(4\pi/15)^{1/2}b_{22,i} \quad (2.10)$$

where u_1 and u_3 are components of the unit vector along the flow and the neutral direction of the flow, respectively.

3. Experimental Section

3.1. Kinetics. The monomers *p*-phenylenediamine (PPD, Aldrich) and terephthaloyl chloride (TPC, Aldrich) are purified by vacuum sublimation under a nitrogen stream to colorless crystals. The solvents *N*-methylpyrrolidone (NMP, Fluka) and hexamethylphosphoramide (HMPA, E. Merck) are purified by vacuum distillation under a nitrogen stream (5 mmHg absolute pressure) and stored over molecular sieves (Raj & Co.) (HMPA has been found to be carcinogenic in rats[16]). The polymerization is carried out in a two-reactor process, as shown in Figure 1.[11] The bottom of the bob in reactor II is conical in shape, with a cone angle such that the shear rate in the cone–plate section is identical to that in the annular gap.

Powdered PPD (0.951 g) is dissolved in the solvent mixture (33 mL of NMP and 11 mL of HMPA) in reactor I, which is then cooled for 10 min to 3 °C. The reaction given below is started by adding 1.786 g of powdered TPC under rapid stirring at 3000 rpm

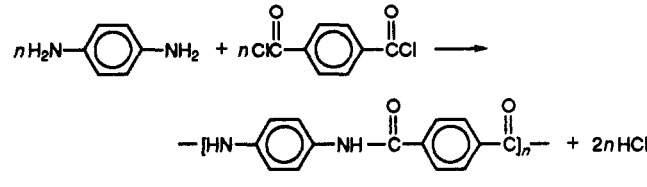

In about 10 s, the temperature of the reaction mixture rises to about 22 °C (Figure 2) and then drops back rapidly to 10 °C in

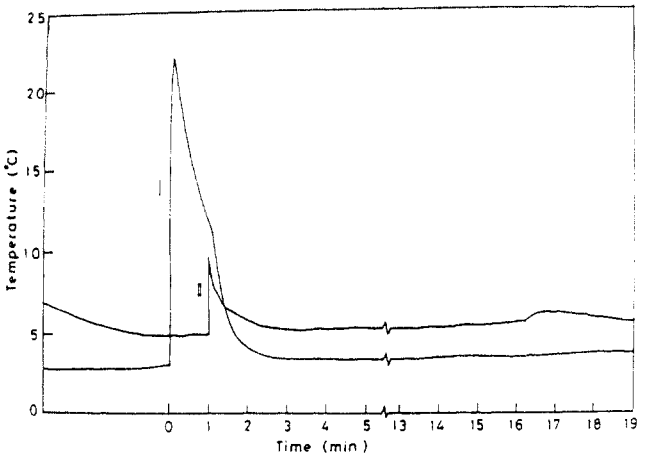

Figure 2. Solution temperature in reactors I and II during polymerization at $\dot{\gamma}$ = 413 s^{-1}.

1 min under continued cooling. At this time, part of the polymerizing mixture is transferred by means of a peristaltic pump to reactor II. Stirring in reactor I is discontinued and the bob of reactor II is rotated at the desired speed. In another minute, the temperatures in reactors I and II reach 3 and 5 °C, respectively, and further polymerization continues in both reactors. Powdering, weighing, and reaction are all carried out in a glovebox in which moisture content has been reduced to less than 100 ppm by drying with air circulation over potassium hydroxide pellets.

The molecular weight at different times is determined by measurement of inherent viscosity (0.5% polymer solution in 98% sulfuric acid at 30 °C) of the polymer obtained by terminating the reaction by mixing with water to precipitate the polymer, followed by vacuum drying at 75 °C. The weight-average molecular weight ($\bar{M}_w$) is calculated using the Mark–Houwink relationship obtained by interpolation of the gel permeation chromatography results of Arpin and Strazielle[15]

$$\bar{M}_w = 3902.39\eta_{inh}^{1.556} \tag{3.1}$$

The weight-average degree of polymerization is then obtained from

$$\overline{DP}_w = \bar{M}_w/238 \tag{3.2}$$

3.2. Birefringence Measurement. The flow birefringence measurements during polymerization under shear are made in the cone–plate section of reactor II. As shown in Figure 1, a polarized He–Ne laser (20 mW, wavelength λ = 632.8 nm, Model 106-A, Spectra-Physics Inc.) beam is directed perpendicular to the plane of the plate at a radial position corresponding to sample thickness a = 1.42 mm. The incident light is polarized at 45° to the flow direction. The polarizing direction of the analyzer is at 90° to that of the polarizer. The birefringence (Δ_{13}) under this configuration is obtained from[1,25]

$$I_\perp = I_0 \sin^2\left(\frac{\pi a \delta_{13}}{\lambda}\right) \tag{3.3}$$

as detailed below. In eq 3.3 I_0 is the total transmitted intensity, and $I_\perp$ is the transmitted intensity measured by the silicon detector (EG&G Model 460–2) and laser power meter (EG&G Gamma Scientific, Model 460–1A) and recorded during polymerization.

During polymerization, as the rigid rodlike polymers grow in size and the rotational diffusivity decreases, orientation of the polymer molecules along the flow direction takes place, and the birefringence Δ_{13} increases. Hence, based on eq 3.3, $I_\perp$ is expected to undergo cyclic changes between maxima (corresponding to $\Delta_{13} = k\lambda/2a$, k = 1, 3, 5, ...) and extinction (corresponding to $\Delta_{13} = k\lambda/2a$, k = 2, 4, 6, ...), the successive maxima in $I_\perp$ being separated by an increase in Δ_{13} of (λ/a). However, due to limitations on the fabrication of the glass conical section, the sample thickness could be controlled only within a tolerance $\pm\delta$. Hence, with the bob rotating, the measured intensity is an average over the intensity due to this variation in sample thickness.

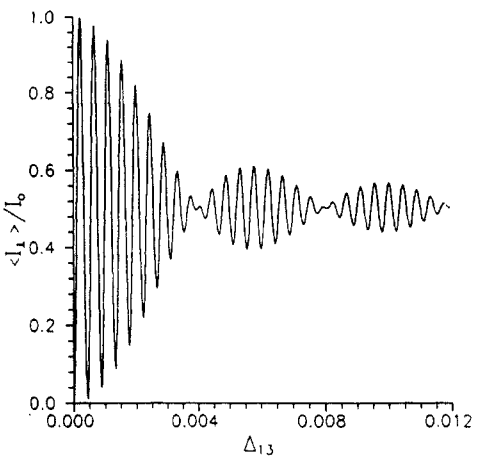

Figure 3. Theoretical estimate of the fractional light transmitted $I_\perp/I_0$ under cross polarization as a function of flow birefringence (eq 3.4) for a = 1.42 mm and $\delta = a/18$.

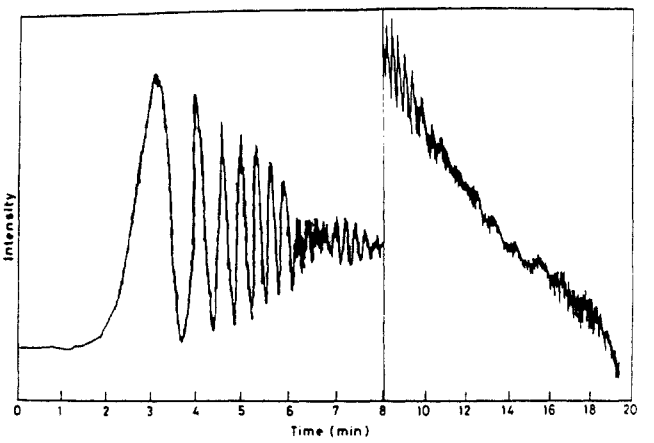

Figure 4. Experimentally measured intensity of transmitted light with crossed polarizers at $\dot{\gamma}$ = 413 s^{-1}. At 8 min the time scale is reduced and the intensity signal amplified.

Assuming a constant probability distribution of thickness variation in this range, we get the average intensity over a complete rotation of the bob to be

$$\langle I_\perp \rangle = I_0\left(\frac{1}{2} - \frac{\lambda}{2\pi\delta\Delta_{13}} \cos\frac{2\pi a\Delta_{13}}{\lambda} \sin\frac{2\pi\delta\Delta_{13}}{\lambda}\right) \tag{3.4}$$

where a quasi-steady-state approximation is made in assuming Δ_{13} constant during a rotation. We plot $I_\perp$ with increase in Δ_{13} in Figure 3. The graph is again cyclic, with the higher frequency cosine peaks enveloped by a lower frequency sine curve. An important distinction of this from the ideal response corresponding to eq 3.3 is that the extinction is never complete. In addition, the amplitude of the oscillations decreases with increasing birefringence. The birefringence variation with time can easily be obtained from an $I_\perp$ versus time trace by noting the time corresponding to the high-frequency peaks and using the fact that the difference in Δ_{13} between successive peaks is (λ/a).

The polymer PPTA is known to exhibit transition to nematic polydomain structure at $c > 8\%$.[26] We have employed $c \sim 6\%$ to avoid phase transition under quiescent conditions as that would lead to additional complications in analysis of results. We have also analyzed for the presence of polydomain structure during polymerization by examination under cross-polarized light, with the polarizer placed parallel to the flow direction.[1] Near-complete extinction throughout the polymerization is obtained with or without flow, implying an absence of a liquid crystalline polydomain structure.

4. Results and Discussion

A sample graph of the variation of $I_\perp$ with time (t) is shown in Figure 4. The graph is qualitatively similar to the calculated curve of the variation of $I_\perp$ with birefrin-

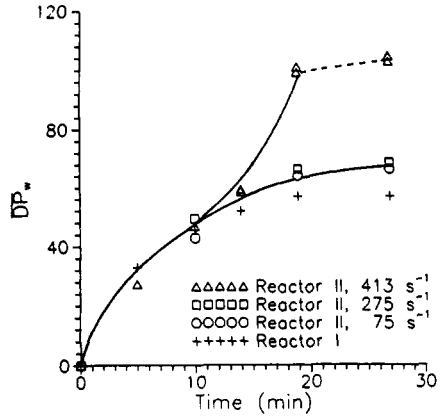

Figure 5. Variation of $\overline{DP}_w$ of PPTA in reactor I and reactor II with time at different shear rates. The full lines are plots of the fitted polynomials (eqs 4.1 and 4.2), and the dashed line indicates the time range during which uniform shear flow could not be maintained.

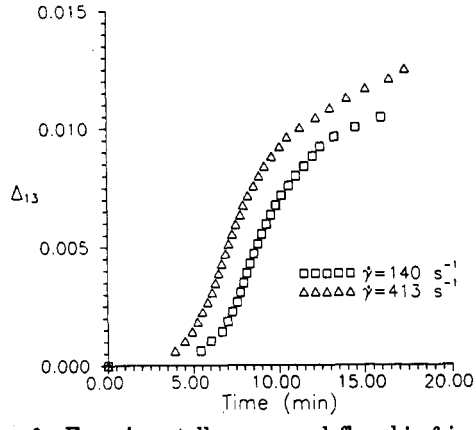

Figure 6. Experimentally measured flow birefringence (Δ_{13}) variation with time of polymerization (t), at two different shear rates ($\dot{\gamma}$).

gence (Figure 3). The corresponding variation of the degree of polymerization ($\overline{DP}_w$) at different shear rates ($\dot{\gamma}$) is presented in Figure 5. The results are similar to those reported earlier[11] but have a lower $\overline{DP}_w$ due to an alternate grade of molecular sieves used for drying the solvents in this set of experiments. (The maximum deviation up to 16 min of reaction is 15%). This is most likely due to the lower efficiency of these sieves in removing moisture from the solvents, which forms a source of chain-terminating side reactions.[10,18,19] In Figure 6 we plot the evolution of birefringence as polymerization proceeds for two different shear rates based on the positions of successive peaks. Beyond t = 16 min, the peaks in $I_\perp$ versus time plots are not distinguishable (Figure 4) due to their reduced amplitude. We find that Δ_{13}, and hence the level of orientation, increases as molecular length increases with time of reaction for both shear rates. At the higher shear rate, the onset of birefringence is attained earlier, or at smaller molecular lengths. The birefringence is also consistently higher for the higher shear rate. Comparison to the kinetics data (Figure 5) shows that the time at which significant increase in the reaction rate occurs also corresponds to the time when the birefringence value is high.

We plot the birefringence variation with $\dot{\gamma}/D_r$ for the two different shear rates to check the scaling law (eq 2.1). With increase in the degree of polymerization the rotational diffusivity decreases, and we calculate the corresponding variation of $\dot{\gamma}/D_r$ with time as follows. $\overline{DP}_w(t)$ is first

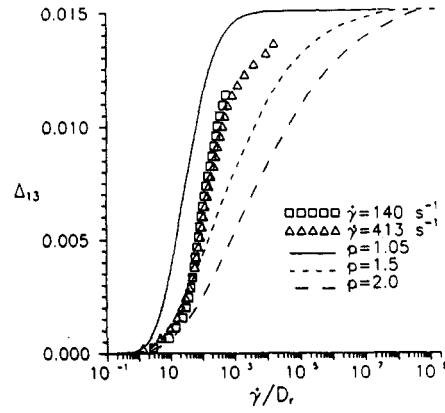

Figure 7. Variation of birefringence (Δ_{13}) with rescaled shear rate ($\dot{\gamma}/D_r$). The symbols denote the experimental data at different shear rates ($\dot{\gamma}$) and the lines the predictions of the DEMG theory for different polydispersity indices (p). The rotational diffusivity (D_r) used to rescale the experimental data is calculated assuming p = 2.

obtained from the following polynomial fits of the data in Figure 5.

$$\overline{DP}_w = 1.02216 + 7.36511t - 0.29003t^2 + 0.00398419t^3 \quad (4.1)$$

for $\dot{\gamma}$ = 75–240 s^{-1}, $0 \le t \le 27$ min, and for $\dot{\gamma}$ = 413 s^{-1}, $0 \le t \le 11.5$ min,

$$\overline{DP}_w = 89.6933 - 8.776t + 0.490667t^2 \quad (4.2)$$

for $\dot{\gamma}$ = 413 s^{-1}, $11.5 < t \le 19$ min. The corresponding D_r for the polydisperse system is obtained assuming the Flory–Schulz[27,28] distribution of molecular weights given by

$$n(L) = \frac{y^z L^{z-1} e^{-yL}}{\Gamma(z)} \quad (4.3)$$

where $n(L)$ is the number density of rods of length L,

$$z = 1/(p-1) \quad (4.4)$$

$$y = (1/\bar{L}_w)\Gamma(z+2)/\Gamma(z+1) \quad (4.5)$$

p is the polydispersity index, $\bar{L}_w$ is the weight-average molecular length, and Γ denotes the gamma function. While we have not shown that the polymer produced follows the above distribution, we use it here for simplicity. In the range of $\overline{DP}_w$ for which Δ_{13} has been measured, i.e., $\overline{DP}_w$ = 35–70, the polydispersity for PPTA is in the range 1.8–2.2.[15,29-31] Though the polydispersity changes during the course of polymerization, this variation in the range of interest is small, and we use p = 2.0 in our calculations. Isotropic diffusivities (D_{ri}) corresponding to Q_{ij} = 1 are then calculated from eq 2.7, with l_{max} = 16, η_s = 5 cP, T = 276 K, $\beta = 1.35 \times 10^3$,[32] and the length of the repeat unit = 12 Å.[15] The above distribution is discretized into 21 divisions, and the representative isotropic diffusivity is given by[6]

$$D_r^{-1} = \frac{\sum_n \rho_n D_{rn}^{-2}}{\sum_n \rho_n D_{rn}^{-1}} \quad (4.6)$$

where ρ_n is the number concentration of molecules of size L_n. Experimental birefringence results in the rescaled form for the two different shear rates are presented in Figure 7. Considering that $\dot{\gamma}/D_r \sim L^7$, so that an error of $2^{1/7} \sim 11\%$ in $\bar{M}_w$ would result in 100% error in calculation of $\dot{\gamma}/D_r$, the two curves may be considered to satisfy the

scaling of eq 2.1 very well. The small deviations may be attributed to (i) uncertainty of the η_{inh}–$\bar{M}_w$ relationship and (ii) differences in polydispersity during polymerization at different shear rates.

The theoretical curves of Δ_{13} variation with $\dot{\gamma}/D_r$ for different values of p are independent of β, $\bar{M}_w$, and $\dot{\gamma}$, and are calculated as follows. For the required polydispersity, the corresponding discretized MWD is obtained as above. Theoretical evaluation of Δ_{13} using eqs 2.9 and 2.10 requires $b_{22,i}$, which can be obtained by solving the matrix equation 2.6. This, however, requires *a priori* knowledge of $\tilde{D}_{ri}$ and Q_{ij}, and hence of $b_{lm,i}$. Thus, an iterative solution procedure is followed. The first approximaion of $\tilde{D}_{ri}$ is taken to be the isotropic diffusivity (D_{ri}), and $b_{lm,i}$ are evaluated. In subsequent iterations Q_{ij} and $b_{lm,i}$ are calculated alternately until $b_{lm,i}$ do not change between successive iterations by more than 0.1%.

The computed results for Flory–Schulz distributions with three different polydispersity indices (p) are plotted in Figure 7. We have used $M = 2.79 \times 10^{-15}$ cm^2, corresponding to the saturation value of $\Delta_{13} = 0.015$, which is inferred from the experimental results. The birefringence becomes detectable at $\dot{\gamma}/D_r \sim 1$, and at large $\dot{\gamma}/D_r$, a saturation in Δ_{13} is reached. The higher slopes of the curves for low-polydispersity cases correspond to a narrow distribution of $\dot{\gamma}/D_r$ in the system. For wider MWD (higher p), the components with widely varying molecular weights orient and contribute to the overall Δ_{13} is widely different ranges of $\dot{\gamma}$. Larger molecules orient at smaller $\dot{\gamma}$, causing early onset of birefringence, while smaller molecules contribute only at much larger $\dot{\gamma}$.

While the theoretical curves are independent of the value of β, the experimental master curve can be moved along the $\dot{\gamma}/D_r$ axis by using suitable values of β, which is determined by the critical concentration for the onset of complete caging. The slope and shape of the master curve cue, however, independent of β. Figure 7 shows that the rate of increase in experimental birefringence with $\dot{\gamma}/D_r$ is much larger than the theoretical curve for a comparable polydispersity. Although Chow et al.[7] reported agreement with the DEMG theory for orientation of collagen molecules in solution under shear, Larson and Mead[27] observed that the DEMG theory was not able to account for the effect of polydispersity on linear viscoelasticity of poly(γ-benzyl L-glutamate) (PBLG) solutions. They attributed the deviation to drastic slowing down of the rotational diffusion of the shorter molecules caused by the matrix of larger molecules. Such an effect would result in a lower value for $\tilde{D}_{ri}$ for the smaller molecules and consequently a steeper increase in Δ_{13}, with $\dot{\gamma}/D_r$. Another contribution to the disagreement between theory and experiment could be the omission of the intermolecular potential term in eq 2.2. Higher levels of intermolecular interaction also result in steeper birefringence vs $\dot{\gamma}$ curves.[33,34] In addition, a preaveraging approximation was used for evaluating the influence of orientation on the rotational diffusivity, which has been reported to lead to errors.[27] Finally, uncertainty in the Mark–Houwink relation used for calculating the molecular weight and the assumed molecular weight distribution would also contribute to the discrepancy between the experimental and theoretical results.

5. Conclusions

During homogeneous solution polymerization of RRL molecules to PPTA under shear flow, significant orientation of molecules takes place, once the molecular lengths are large enough. The onset of detectable orientation occurs at smaller rod lengths and remains consistently higher at the higher shear rate. The evolution of the birefringence is found to depend on $\dot{\gamma}/D_r$ for different shear rates, confirming the scaling law given in eq 2.1.

A comparison of the experimental results with theoretical predictions shows a considerable difference between the two, which could be due to one or more of the following: (i) the DEMG theory is not able to effectively account for the reduction in the rotational motion of small molecules caused by the presence of the larger molecules, (ii) the intermolecular potential has been neglected in this analysis, (iii) the preaveraging approximation has been used in obtaining the D_r dependence on orientation, and (iv) there is an uncertainty associated with the value of the exponent in the η_{inh}–$\bar{M}_w$ relationship and the measurements of the MWD.

The validity of the scaling relationship during polymerization suggests that birefringence measurements could be used as a rapid, on-line method for monitoring the extent of reaction of rodlike molecules during commercial polymerization processes. The results also have implications for the design of reactors for polymerization of rodlike molecules. Since molecular orientation, rather than mixing, is responsible for higher polymerization rates during the slow, diffusion-controlled phase of polymerization, the geometry of the reactor for this stage should be chosen appropriately to achieve this. For example, an annular geometry to produce a simple shear flow with a sufficiently high shear rate could suffice for late stages of the polymerization instead of the complex designs that are used in practice.[16]

References and Notes

(1) Asada, T.; Muramatsu, H.; Watanabe, R.; Onogi, S. *Macromolecules* **1980**, *13*, 867.
(2) Ernst, B.; Navard, P.; Hashimoto, T.; Takebe, T. *Macromolecules* **1990**, *23*, 1370.
(3) Takebe, T.; Hashimoto, T.; Ernst, B.; Navard, P.; Stein, R. S. *J. Chem. Phys.* **1990**, *92*, 1386.
(4) Srinivasrao, M.; Berry, G. C. *J. Rheol.* **1991**, *35*, 379.
(5) Tsvetkov, V. N.; Shtennikova, I. N.; Peker, T. V.; Kudriavtsev, G. I.; Volokhina, A. V.; Kalmykova, V. D. *Eur. Polym. J.* **1977**, *13*, 455.
(6) Chow, A. W.; Fuller, G. G. *Macromolecules* **1985**, *18*, 786.
(7) Chow, A. W.; Fuller, G. G.; Wallace, D. G.; Madri, J. A. *Macromolecules* **1985**, *18*, 793, 805.
(8) Chu, S. G.; Venkatraman, S.; Berry, G. C.; Einaga, Y. *Macromolecules* **1981**, *14*, 939.
(9) Cotts, D. B.; Berry, G. C. *Macromolecules* **1981**, *14*, 930.
(10) Jingshen, B.; Anji, Y.; Shengqing, Z.; Shufan, Z.; Chang, H. *J. Appl. Polym. Sci.* **1981**, *26*, 1211.
(11) Agarwal, U. S.; Khakhar, D. V. *Nature* **1992**, *360*, 53.
(12) Agarwal, U. S.; Khakhar, D. V. *J. Chem. Phys.* **1992**, *96*, 7125.
(13) Doi, M.; Edwards, S. F. *J. Chem. Soc., Faraday Trans.* **1978**, *74*, 560, 918.
(14) Morgan, P. W. *Macromolecules* **1977**, *10*, 1381.
(15) Arpin, M.; Strazielle, C. *Polymer* **1977**, *18*, 591.
(16) Vollbracht, L. In *Comprehensive Polymer Science*; Allen, G., Bevington, J. C.; Eds.; Pergamon Press: Oxford, 1989; Vol. 5, p 375.
(17) PPTA has a persistence length of 150–450 Å and hence is a very stiff molecule at the length scale of a single bond. Since sharp bends (radius of curvature O(1 bond length)) are not likely, bond formation between oligomers which are not already aligned is improbable.
(18) Herlinger, H.; Hoerner, H.; Druschke, F.; Denneler, W.; Haiber, F. *Appl. Polym. Symp.* **1973**, *21*, 201.
(19) Morgan, P. W. *Condensation Polymers by Interfacial and Solution Methods*; Interscience: New York, 1965.
(20) Marrucci, G.; Grizzuti, N. *J. Polym. Sci., Polym. Lett. Ed.* **1983**, *21*, 83.
(21) Mead, D. W.; Larson, R. G. *Macromolecules* **1990**, *23*, 2524.
(22) Doi, M.; Edwards S. F. *The Theory of Polymer Dynamics*; Clarendon Press: Oxford, 1986; p 324.

(23) Lebedev, A. V.; Federova, R. M. *A Guide to Mathematical Tables*; Pergamon Press: Oxford, 1960.
(24) Yamakawa, H. *Modern Theory of Polymer Solutions*; Harper and Row Publishers: New York, 1971.
(25) Kimura, S.; Osaki, K.; Kurata, M. *J. Polym. Sci.* **1970**, *19*, 156.
(26) Bair, T. I.; Morgan, P. W.; Killian, F. L. *Macromolecules* **1977**, *10*, 1396.
(27) Larson, R. G.; Mead, D. W. *J. Polym. Sci., Polym. Phys. Ed.* **1991**, *29*, 1271.
(28) Zimm, B. H. *J. Chem. Phys.* **1948**, *16*, 1099.
(29) Ogata, N.; Sanui, K.; Kitayama, S. *J. Polym. Sci., Polym. Chem. Ed.* **1984**, *22*, 865.
(30) Roche, E. J.; Allen, S. R.; Gabara, V.; Cox, B. *Polymer* **1989**, *60*, 1776.
(31) Chu, B.; Ying, Q.; Wu, C.; Ford, J. R.; Dhalal, H. S. *Polymer* **1985**, *26*, 1408.
(32) Teraoka, I.; Hayakawa, R. *J. Chem. Phys.* **1989**, *91*, 2643.
(33) Bahar, I.; Erman, B. *J. Polym. Sci., Polym. Phys. Ed.* **1986**, *24*, 1361.
(34) See, H.; Doi, M.; Larson, R. *J. Chem. Phys.* **1990**, *92*, 792.